

# Research on a novel nonlinear conformable fractional accumulation kernel GM (1, N) model

Shaoyong Liu

College of Mathematics and Computer Science, Tongling University, Tongling, 244061, China

**Abstract:** Grey system theory is widely used to deal with the uncertainty caused by partially known information. Grey time series analysis plays an important role in decision-making and forecasting, of which grey forecasting is the key branch. The traditional grey multivariable model is limited to be widely used in practical application because of its lack of prediction accuracy and poor adaptability. Kernel Methods is a powerful pattern recognition algorithm in machine learning, which is particularly good at dealing with nonlinear multivariable models. A novel nonlinear conformable fractional accumulation kernel grey GM (1, N) model on account of the kernel method (abbreviated as CFAKGM (1, N)) is arranged in this work to improve the prediction accuracy. Furthermore, the utilization of conformable fractional accumulation enhances the prediction accuracy of the model, and the model's hyperparameters are determined through the application of the four vectors intelligent metaheuristic method (abbreviated as FVIM). Numerical investigations demonstrate that when processing the prediction of complex systems, the CFAKGM (1, N) model may capture the nonlinear dynamic properties of the data more effectively and enhance the prediction accuracy significantly.

**Keywords:** Multivariate Grey Model, Kernel Method, Four Vector Intelligent Metaheuristic

## 1. Introduction

Theoretically more significant than GM (1,1), GM (1, N) is a multivariate grey model that takes a more comprehensive approach, making it more general than GM (1,1). However, Zhang [1] reported that the method of GM (1, N) was incorrect, and put out the GMC (1, N) first-order multivariable gray model, which is more accurate[2]. The modeling process of GMC (1, N) model actually represents a new multivariate gray model modeling method. For example, the grey models of DVCGM (1, N)[3] is similar to the modeling process of GMC (1, N). In the broad field of exploring multivariate grey prediction models, KGM (1, N) is established under the principle of structural risk minimization[4]. It is worth noting that KGM (1, N) contains a nonlinear function estimated by a kernel function, which can be theoretically approximated as any continuous function. Hence, for the regularization and kernel parameters [5] that influence the stability of the KGM (1, N) model, a minute alteration in these parameters can result in varied predictive outcomes. Consequently, the KGM (1, N) model is well-suited for fractional cumulative generation.

In grey system theory, the cumulative generation operator is a way to whiten grey processes in order to reduce fluctuations and enhance regularity. In 2014, Khalil et al.[6] introduced a novel conceptualization of the fractional derivative, termed the compatible fractional derivative. This new definition of a derivative is significantly more straightforward compared to the conventional definitions of fractional derivatives, such as the Riemann-Liouville and Caputo definitions. Khalil and colleagues demonstrated that compatible fractional derivatives possess advantageous properties and are capable of addressing numerous challenges that were previously formidable or insurmountable when employing the traditional definitions. Owing to these substantial advancements, compatible fractional derivatives have garnered considerable attention from the research community in recent years, leading to the emergence of significant new findings. Using the fractional cumulative generation method, the disturbance boundary can be reduced. In addition, the contradiction between the result that new data have little impact on the solution and the new information priority principle is alleviated.

The task of optimizing the optimal fractional order  $\alpha$  involves identifying the most suitable parameter to minimize the mean absolute percentage error (abbreviated as MAPE) of the model. This optimization task fundamentally represents a non-linear programming issue, characterized by an objective function and constraints that display non-linear properties. Numerous nonlinear optimization algorithms have been employed for grey system models in recent scholarly works. Additionally, heuristic

methods are frequently utilized to address analogous problems in various other domains[7]. The FVIM algorithm addresses prevalent challenges in optimization problems, including convergence instability, entrapment in local optima, and the identification of optimal solutions, as well as the complexities faced by real-world optimization processes. The FVIM methodology is distinguished by its dependence on the four most promising positions within the swarm to direct the swarm's movement. Moreover, the algorithm incorporates an innovative vector position, calculated as the arithmetic mean of these four optimal points, which has the potential to yield solutions surpassing those previously identified. This method enhances the particles' exploratory capabilities within the search domain, thereby improving swarm exploration and exploitation. Consequently, it increases the probability of locating the global optimum while mitigating the risk of converging to local minima.

On these theoretical bases, the article proposed a novel nonlinear uniform fractional order kernel GM (1, N) model. The primary contributions are summarized as follows:

(1) The FVIM method is employed to increase the generalization power and handle the overfitting problem by combining base learners and kernel-based nonlinear multivariate grey models in a conformable fractional approach to generate a composite predictor.

(2) Experimental results show that CFAKGM (1, N) outperforms the comparison models in terms of predictive accuracy when forecasting different datasets.

The structure of the remainder of this manuscript is as follows. Section 2 delineates the KGM (1, N) model. Section 3 presents the CFAKGM (1, N) model. Section 4 outlines the optimization of parameters. Section 5 showcases the empirical forecasting outcomes for various datasets and juxtaposes the forecasting performance of the CFAKGM (1, N) model against other models. Section 6 concludes the study.

## 2. The KGM (1, N) model

This part provides a succinct synopsis of the KGM (1, N) model and its associated mathematical underpinnings.

The KGM (1, N) model primarily focuses on a grey system characterized by a series of  $n$  elements  $(X_1^{(0)}, X_2^{(0)}, \dots, X_n^{(0)})$ , where  $X_1^{(0)}$  is designated as the output series, and  $X_u^{(0)}$  (with  $u$  elements ranging from 2 to  $n$ ) are considered as the input series. The first-order accumulative generation operation (abbreviated as 1-AGO) is defined as follows

$$X_u^{(1)}(k) = \sum_{v=1}^k X_u^{(0)}(v), (u = 1, 2, \dots, N). \tag{1}$$

The background value, denoted as  $M_1^{(1)}$ , is also termed the mean sequence generated by consecutive neighbors of  $X_1^{(1)}$ , as described in reference [8]. It is defined as follows

$$M_1^{(1)}(k) = 0.5(X_1^{(1)}(k) + X_1^{(1)}(k - 1)). \tag{2}$$

It is evident that the OGM (1, N) model is inherently linear, focusing solely on the linear correlation between the input and output sequences. To endow the model with nonlinear characteristics, it is imperative to incorporate a nonlinear function of the input sequence. Consequently, the nonlinear form of the KGM (1, N) model can be derived as follows

$$X_1^{(0)}(k) + aM_1^{(1)}(k) = \phi(k) + b, \tag{3}$$

where  $\phi(k)$  represents a nonlinear function of the input series  $(X_2^{(0)}, \dots, X_n^{(0)})$ , and  $b$  is a bias term. In accordance with the kernel method, feature mapping is employed to project the input sequence into a higher-dimensional feature space as  $\varphi : R^{n-1} \rightarrow H$ .

Subsequently, the nonlinear function  $\phi(k)$  can be linearized in the feature space, expressed as

$$\phi(k) = \mathbf{w}^T \boldsymbol{\varphi}(\chi(k)), \tag{4}$$

where  $\chi(k) = [X_2^{(1)}(k), \dots, X_n^{(1)}(k)]^T$ , and  $\mathbf{w} \in \mathbb{H}$  as a weight vector, respectively.

In practical scenarios, it is often computationally impractical to ascertain the precise nonlinear mapping  $\boldsymbol{\varphi}$  from Eq. (4). As a result, the parameters of the KGM (1, N) model cannot be estimated using the least squares method. Consequently, the following regularization problem is considered

$$\begin{aligned} \min_{a, \mathbf{w}, \mathbf{e}} J(a, \mathbf{w}, \mathbf{e}) &= \frac{a^2}{2} + \frac{\mathbf{w}^2}{2} + \frac{C}{2} \sum_{v=2}^m \mathbf{e}_k^2, \\ \text{s.t. } \mathbf{e}_k &= X_1^{(0)}(k) + aM_1^{(1)}(k) - \mathbf{w}^T \boldsymbol{\varphi}(\chi(k)) - b, \end{aligned} \tag{5}$$

where  $C$  is designated as the regularized parameter, which governs the equilibrium between the fitting error and the smoothness of the generated series. The quadratic regularization term in Eq. (5) constitutes a semi-parametric approach frequently employed in partially linear Least Squares Support Vector Machines (LSSVMs). This formulation is analogous to that of ridge regression[9].

To address this issue, it is essential to initially formulate the Lagrangian function corresponding to Eq. (5) as

$$L := \frac{a^2}{2} + \frac{\mathbf{w}^2}{2} + \frac{C}{2} \sum_{k=2}^r \mathbf{e}_k^2 + \sum_{k=2}^m \lambda_k [X_1^{(0)}(k) + aM_1^{(0)}(k) - \mathbf{w}^T \boldsymbol{\varphi}(\chi(k)) - b - \mathbf{e}_k], \tag{6}$$

where  $\lambda_k$  represent the Lagrangian multipliers. Subsequently, the Karush-Kuhn-Tucker (KKT) conditions are outlined as follows

$$\begin{cases} \frac{\partial L}{\partial a} = 0 \Rightarrow a = -\sum_{k=2}^m \lambda_k M_1^{(1)}(k) \\ \frac{\partial L}{\partial \mathbf{w}} = 0 \Rightarrow \mathbf{w} = \sum_{k=2}^m \lambda_k \boldsymbol{\varphi}(\chi(k)) \\ \frac{\partial L}{\partial \mathbf{e}_k} = 0 \Rightarrow \mathbf{e}_k = \lambda_k / C \\ \frac{\partial L}{\partial u} = 0 \Rightarrow \sum_{k=2}^m \lambda_k = 0 \\ \frac{\partial L}{\partial \lambda_j} = 0 \Rightarrow X_1^{(0)}(k) + aM_1^{(0)}(k) - \mathbf{w}^T \boldsymbol{\varphi}(\chi(k)) - b = \mathbf{e}_k \end{cases} . \tag{7}$$

By eliminating the  $a$ ,  $\mathbf{w}$  and  $\mathbf{e}_k$ , the linear system, in essence, mirrors the KKT conditions, as articulated below:

$$\begin{pmatrix} 0 & \mathbf{1}_{m-1}^T \\ \mathbf{1}_{m-1} & \boldsymbol{\Omega} + \mathbf{I}_{m-1}/C \end{pmatrix} \begin{pmatrix} b \\ \boldsymbol{\lambda} \end{pmatrix} = \begin{pmatrix} 0 \\ Y \end{pmatrix}, \tag{8}$$

where

$$\mathbf{1}_{m-1} = [1, 1, \dots, 1]_{m-1}^T, \boldsymbol{\lambda} = [\lambda_1, \lambda_2, \dots, \lambda_m]^T,$$

$$\Omega = \left( \varphi(\chi(u)) \cdot \varphi(\chi(v)) - M_1^{(1)}(u) M_1^{(1)}(v) \right)_{(m-1) \times (m-1)}, Y = \left[ X_1^{(0)}(2), X_1^{(0)}(3), \dots, X_1^{(0)}(m) \right]^T,$$

and  $I_{m-1}$  is an  $m-1$  dimensional identity matrix. The parameter  $\alpha$  can be determined by solving the first equation derived from the KKT conditions, alongside the resolution of the linear system.

It can be seen that without knowing the expression of the eigenmap  $\varphi$ , this work can use the value of the inner product  $\varphi(X(u)) \cdot \varphi(X(v))$  to solve the linear system. So, through the kernel function:

$$K(\chi(u), \chi(v)) = \varphi(\chi(u)) \cdot \varphi(\chi(v)). \tag{9}$$

In this study, the focus is on the Gaussian kernel function, which is widely used and generally expressed as

$$K(\chi(u), \chi(v)) = \exp \left\{ -\frac{\|\chi(u) - \chi(v)\|^2}{2\sigma^2} \right\}, \tag{10}$$

where  $\|\cdot\|$  denotes the Euclidean norm of the vectors, and  $\sigma$  represents the kernel parameter. Subsequently, the linear system in Eq. (8) can be resolved utilizing the Gaussian kernel.

Given the second equation  $w = \sum_{k=2}^m \lambda_k \varphi(X(k))$  of the KKT conditions in Eq. (7) and the definition of  $\phi(k)$  in Eq. (3), it follows

$$\phi(k) = w^T \varphi(k) = \sum_{j=2}^m \lambda_j \varphi(\chi(u)) \cdot \varphi(\chi(k)). \tag{11}$$

A kernel function can be used to express the inner products  $\varphi(X(v)) \cdot \varphi(X(k))$ . As a result, the nonlinear function  $\phi(k)$  can be represented by substituting the kernel function into Eq. (11) in the following manner.

$$\phi(k) = w^T \varphi(k) = \sum_{j=2}^m \lambda_j K(\chi(v), \chi(k)). \tag{12}$$

By incorporating the parameters  $\lambda_2, \lambda_3, \dots, \lambda_m$  and an appropriate kernel function (such as the Gaussian kernel, as exemplified in Eq. (10)), reaching a point where it is possible to computationally assess the nonlinear function  $\phi(k)$ .

The resolution of the KGM (1, N) model parallels that of the OGM (1, N). By integrating Eq. (2) into the KGM (1, N) model Eq. (3), it follows that

$$X_1^{(1)}(k) = \alpha X_1^{(1)}(k-1) + \psi(k) + \mu, \tag{13}$$

where

$$\alpha = \frac{1-0.5a}{1+0.5a}, \psi(k) = \frac{\phi(k)}{1+0.5a}, \mu = \frac{b}{1+0.5a}. \tag{14}$$

By solving the Eq. (13) recursively, the KGM (1, N) response function as shown below

$$\hat{X}_1^{(1)}(k) = \alpha^{k-1} \hat{X}_1^{(0)}(1) + \sum_{\tau=2}^k (\psi(\tau) + \mu) \cdot \alpha^{k-\tau}. \tag{15}$$

As per Eq. (12), the response function enables the computation of the 1-AGO series. Subsequently, the reconstructed values can be retrieved by employing the 1-IAGO as

$$\hat{X}_1^{(0)}(k) = \hat{X}_1^{(1)}(k) - \hat{X}_1^{(1)}(k-1). \tag{16}$$

### 3. The proposed conformable fractional accumulation kernel grey GM (1, N) model

This section mainly introduces the newly proposed conformable fractional accumulation kernel grey GM (1, N) model.

#### 3.1 The conformable fractional order accumulation operator

The formulation of the conformable fractional order accumulation is derived from the definition of the conformable fractional derivative. This definition can be expressed as follows:

Definition 1 (See[10]). For  $\forall t > 0, \alpha \in (0, 1]$ , there exists a differentiable function  $\exists f : [0, \infty) \rightarrow R$ , then the  $\alpha$  order corresponding fractional derivative of  $f$  can be expressed as

$$B_\alpha(f)(t) = \lim_{\varepsilon \rightarrow 0} \frac{f(t + \varepsilon t^{1-\alpha}) - f(t)}{\varepsilon}. \tag{17}$$

Definition 2. For  $\forall k \in N^+, \alpha \in (0, 1]$ , the conformable fractional difference (CFD) of order  $f$  of  $\alpha$  order can be expressed as

$$\Delta^\alpha f(k) = k^{1-\alpha} \Delta f(k) = k^{1-\alpha} [f(k) - f(k-1)], \tag{18}$$

Definition 3. For  $\forall k \in N^+, \alpha \in (0, 1]$ , the conformable fractional accumulation (CFA) of  $f$  with  $\alpha$  order can be represented as

$$\nabla^\alpha f(k) = \nabla \left( \frac{f(k)}{k^{1-\alpha}} \right) = \sum_{j=1}^k \left( \frac{f(j)}{j^{1-\alpha}} \right), \tag{19}$$

Definition 4.  $\forall n \in N$ , the  $\alpha$  order  $(\alpha \in (n, n+1])$  CFD can be represented as

$$\Delta^\alpha f(k) = k^{[\alpha]-\alpha} \Delta^n f(k). \tag{20}$$

Clearly, when  $\alpha = 1$  approaches infinity, it yields the  $n+1$  order difference  $\Delta^{n+1}$ . Including  $\alpha = 0$ , Definition 4 constitutes a universal definition of the conformable fractional derivative (CFD), as it applies to all nonnegative integers  $\alpha$ .

It is worth noting that higher order CFA is still the inverse operator of higher order CFD, i.e.  $\forall \alpha \in (n, n+1], \Delta^\alpha \nabla^\alpha f(k) = f(k)$ . Recalling Definition 4, it can be deduced

$$k^{[\alpha]-\alpha} \Delta^n \nabla^\alpha f(k) = f(k). \tag{21}$$

Similarly, the definition of the  $\alpha$  order conformable fractional average (CFA) can be derived by dividing Eq. (31) by  $k^{[\alpha]-\alpha}$  and leveraging the correlation  $\Delta^n \nabla^\alpha f(k) = f(k)$ .

Definition 5. The  $\alpha$  order  $(\alpha \in (n, n+1])$  CFA can be represented as

$$\nabla^\alpha f(k) = \nabla^\alpha \left( \frac{f(k)}{k^{[\alpha]-\alpha}} \right). \tag{22}$$

When  $\alpha = n + 1$ , the (CFA yields the  $(n + 1)$  order accumulation  $\nabla^{n+1}$ . Similarly, including  $\alpha = 0$ , Definition 5 represents a universal definition for the CFA, as it applies to all nonnegative integers  $\alpha$ . Using the uniform definition of CFA, it is easy to derive the recursive equation as

$$\nabla^\alpha f(k) = \nabla \left( \nabla^{n-1} \left( \frac{f(k)}{k^{[\alpha]-\alpha}} \right) \right) = \sum_{j=1}^k (\nabla^{\alpha-1} f(j)), \alpha \geq 1, \tag{23}$$

and  $n = [\alpha] - 1$ . The formula is very convenient for computer operation.

### 3.2 The CFAKGM (1, N) model

In this work, CFAKGM (1, N) is proposed within the context of CFA and CFD definitions, and pertinent procedures are illustrated in this part.

First, indicate the  $\alpha$  order CFA as

$$X^{(\alpha)} = (x^{(\alpha)}(1), x^{(\alpha)}(2), \dots, x^{(\alpha)}(N)), \tag{24}$$

where

$$X^{(\alpha)}(k) = \nabla^\alpha x^{(0)}(k) = \begin{cases} \sum_{j=1}^k \frac{x^{(0)}(j)}{j^{[\alpha]-\alpha}}, & 0 < \alpha \leq 1. \\ \sum_{j=1}^k x^{(\alpha-1)}(j), & \alpha > 1. \end{cases} \tag{25}$$

The background value  $M_1^{(\alpha)}$  is expressed as

$$M_1^{(\alpha)}(k) = 0.5 (X_1^{(\alpha)}(k) + X_1^{(\alpha)}(k-1)). \tag{26}$$

Hence, the nonlinear expression of the CFAKGM (1, N) model could be formulated as

$$X_1^{(0)}(k) + aM_1^{(\alpha)}(k) = \phi(k) + b, \tag{27}$$

where  $\phi(k)$  represents a nonlinear function of the input series  $(X_2^{(0)}, \dots, X_n^{(0)})$ , and  $b$  is a bias term. Subsequently, the nonlinear function  $\phi(k)$  can be linearized in the feature space, expressed as

$$\phi(k) = \mathbf{w}^T \varphi(\chi(k)), \tag{28}$$

where  $\mathbf{w} \in \mathbb{H}$  is a weight vector,  $\chi(k) = [X_2^{(\alpha)}(k), \dots, X_n^{(\alpha)}(k)]^T$ .

### 3.3 Parameters estimation of the CFAKGM (1, N)

In practice, it is frequently computationally intractable to determine the exact nonlinear mapping  $\phi$  from Eq. (29). Therefore, the parameters of the CFAKGM (1, N) model cannot be determined using the least squares approach. Instead, the following regularization issue is addressed

$$\min_{a,w,e} J(a, w, e) = \frac{a^2}{2} + \frac{w^2}{2} + \frac{C}{2} \sum_{v=2}^m e_k^2,$$

$$s.t. e_k = X_1^{(0)}(k) + aM_1^{(\alpha)}(k) - w^T \phi(\chi(k)) - b, \tag{29}$$

where  $C$  is referred to as the regularized parameter, which regulates how well the resulting series balances the fitting error and its flatness. To address this issue, as above, define the Lagrangian as

$$L := \frac{a^2}{2} + \frac{w^2}{2} + \frac{C}{2} \sum_{k=2}^r e_k^2 + \sum_{k=2}^m \lambda_k \left[ X_1^{(0)}(k) + aM_1^{(\alpha)}(k) - w^T \phi(\chi(k)) - e_k - b \right], \tag{30}$$

where  $\lambda_k$  is the Lagrangian multipliers. The linear system, in essence, mirrors the KKT conditions, as articulated below

$$\begin{pmatrix} 0 & 1_{m-1}^T \\ 1_{m-1} & \Omega + I_{m-1}/C \end{pmatrix} \begin{pmatrix} b \\ \lambda \end{pmatrix} = \begin{pmatrix} 0 \\ Y \end{pmatrix}, \tag{31}$$

where

$$\Omega = \left( \phi(\chi(u)) \cdot \phi(\chi(v)) - M_1^{(\alpha)}(u) M_1^{(\alpha)}(v) \right)_{(m-1) \times (m-1)}.$$

The KGM (1, N) and the CFAKGM (1, N) solutions are similar in how they work. Solving the (12) repeatedly yields the response function of the CFAKGM (1, N).

$$\hat{X}_1^{(\alpha)}(k) = \alpha^{k-1} \hat{X}_1^{(0)}(1) + \sum_{\tau=2}^k (\psi(\tau) + \mu) \cdot \alpha^{k-\tau}. \tag{32}$$

The CFD can still be used to acquire the recovered data as

$$\hat{X}_1^{(0)}(k) = k^{[\alpha]-\alpha} \left( \hat{X}_1^{(\alpha)}(k) - \hat{X}_1^{(\alpha)}(k-1) \right). \tag{33}$$

#### 4. Determining the Conformable Fractional Accumulation Kernel Grey GM (1, N) Model With Four Vector Intelligent Metaheuristic Algorithm

In this section, using an intelligent optimization method, the FVIM algorithm, to find the optimal solution of the nonlinear parameter  $\alpha$ .

##### 4.1 Model Evaluation Criteria

In this study use MAPE as the objective function of the FVIM algorithm and find the parameter combination that minimizes MAPE through iterative updates.

Table 1: The evaluation criteria.

| MAPE (%) | Prediction Performance |
|----------|------------------------|
| < 10     | Wonderful              |
| 10 – 20  | Great                  |
| 20 – 50  | Logical                |
| >50      | Incorrect              |

In each iteration, the FVIM algorithm updates the positions of the other individuals based on the four best-performing individuals in the current population, while using Gaussian kernel functions to deal with nonlinear relationships in the input data. According to Table 1 for details.

##### 4.2 The Four Vector Intelligent Metaheuristic Algorithm

Algorithm 1. Algorithm of FVIM to search for the nonlinear parameter  $\alpha$  of the grey model.

|  |
|--|
| <p>Input: Number of agents <math>n, z = \{1, 2, 3, 4\}</math>, dimensions <math>d</math>, objective function <math>f(x)</math>, Max iterations <math>r</math>.</p> <p>Output: The best solution <math>P_{best}</math>.</p>   |
| <p>1: Initialize: the four vector population <math>X_i (i = 1, 2, \dots, n)</math> in the swarm randomly, initialize the four agent positions <math>P_1, P_2, P_3, P_4</math></p> <p>2: For <math>i = 1</math> to <math>n</math> do</p> <p>3:   Evaluate the fitness <math>f(X_i)</math> of each agent</p> <p>4: End for</p> <p>5: Identify the four best-performing agents <math>P_1, P_2, P_3, P_4</math></p> <p>6: For <math>j = 1</math> to <math>n</math> do</p> <p>7:   For <math>i = 1</math> to <math>n</math> do</p> <p>8:     Update using equations (34) to (37)</p> <p>9:     Update the average position <math>\bar{P}_i</math> using equation (38)</p> <p>10:   End for</p> <p>11:   Identify the four best-performing agents <math>P_1, P_2, P_3, P_4</math></p> <p>12:   Evaluate the fitness <math>f(X_i)</math> of each agent</p> <p>13: End for</p> |

Algorithm 1 delineates a sequential process that encompasses all crucial parameters required for the identification of the optimal solution. The FVIM algorithm utilizes unique mathematical models to control how the search agents behave. These models include four different equations for how the agents move and position themselves (Equations 34-37). The localization update mechanism amalgamates a plethora of elements that influence the navigational trajectory and progression of each agent throughout the optimization process, as depicted by the subsequent equations.

$$\begin{cases} X_{1,i} = P_{1,i} + (2 \times \alpha \times \xi_1 - \alpha) \times |\xi_2 \times P_{1,i} - \bar{P}_i|, \text{if } \xi_3 < 0.5 \\ X_{1,i} = P_{1,i} - (2 \times \alpha \times \xi_1 - \alpha) \times |\xi_2 \times P_{1,i} - \bar{P}_i|, \text{otherwise} \end{cases} \quad (34)$$

$$\begin{cases} X_{2,i} = P_{2,i} + (2 \times \alpha \times \xi_1 - \alpha) \times |\xi_2 \times P_{2,i} - \bar{P}_i|, \text{if } \xi_3 < 0.5 \\ X_{2,i} = P_{2,i} - (2 \times \alpha \times \xi_1 - \alpha) \times |\xi_2 \times P_{2,i} - \bar{P}_i|, \text{otherwise} \end{cases} \quad (35)$$

$$\begin{cases} X_{3,i} = P_{3,i} + (2 \times \alpha \times \xi_1 - \alpha) \times |\xi_2 \times P_{3,i} - \bar{P}_i|, \text{if } \xi_3 < 0.5 \\ X_{3,i} = P_{3,i} - (2 \times \alpha \times \xi_1 - \alpha) \times |\xi_2 \times P_{3,i} - \bar{P}_i|, \text{otherwise} \end{cases} \quad (36)$$

$$\begin{cases} X_{4,i} = P_{4,i} + (2 \times \alpha \times \xi_1 - \alpha) \times |\xi_2 \times P_{4,i} - \bar{P}_i|, \text{if } \xi_3 < 0.5 \\ X_{4,i} = P_{4,i} - (2 \times \alpha \times \xi_1 - \alpha) \times |\xi_2 \times P_{4,i} - \bar{P}_i|, \text{otherwise} \end{cases} \quad (37)$$

$$\bar{P}_i = (X_{1,i} + X_{2,i} + X_{3,i} + X_{4,i}) / 4 \quad (38)$$

In the context of the algorithm,  $\bar{P}_i$  is an adaptive coefficient, represents the current average position of all agents in  $i$  dimension.  $X_{n,i}$  signifies the updated position for the  $n^{th}$  best agent in the  $i$



dimension.  $P_{n,i}$  denotes the current position of the  $n^{th}$  best agent in  $i$  dimension.  $\xi_1, \xi_2, \xi_3$  denotes random variables that are uniformly distributed within the interval  $[0,1]$ . The incorporation of random numbers  $\xi_1$  and  $\xi_2$  into the algorithm introduces stochasticity, thereby ensuring that agents explore a wide array of regions within the search space and avoid converging to local minima.

**5. Application**

In this section, the validations are performed to examine the predictive advantage of the proposed CFAKGM (1, N) model through a real-world example. The first dataset in this work is the cumulative GDP cumulative year-on-year for Shanghai, Anhui, Jiangsu and Zhejiang from September 2018 to June 2024. The data is illustrated in the Table 2 come from Wind.

Table 2: The raw data.

| Date  | Shang Hai $X_2^{(0)}$ | An Hui $X_3^{(0)}$ | Jian Su $X_4^{(0)}$ | Zhe Jiang $X_1^{(0)}$ | Date  | Shang Hai $X_2^{(0)}$ | An Hui $X_3^{(0)}$ | Jian Su $X_4^{(0)}$ | Zhe Jiang $X_1^{(0)}$ |
|-------|-----------------------|--------------------|---------------------|-----------------------|-------|-----------------------|--------------------|---------------------|-----------------------|
| 18.09 | 6.80                  | 8.20               | 6.70                | 7.50                  | 21.09 | 9.80                  | 10.20              | 10.20               | 10.60                 |
| 18.12 | 6.80                  | 8.00               | 6.70                | 7.10                  | 22.12 | 8.10                  | 8.30               | 8.60                | 8.50                  |
| 19.03 | 5.70                  | 7.70               | 6.70                | 7.70                  | 22.03 | 3.10                  | 5.20               | 4.60                | 5.10                  |
| 19.06 | 5.90                  | 8.00               | 6.50                | 7.10                  | 22.06 | -5.70                 | 3.00               | 1.60                | 2.50                  |
| 19.09 | 6.00                  | 7.80               | 6.40                | 6.60                  | 22.09 | -1.40                 | 3.30               | 2.30                | 3.10                  |
| 19.12 | 6.00                  | 7.50               | 6.10                | 6.80                  | 22.12 | -0.20                 | 3.50               | 2.80                | 3.10                  |
| 20.03 | -6.70                 | -6.50              | -5.00               | -5.60                 | 23.03 | 3.00                  | 4.80               | 4.70                | 4.90                  |
| 20.06 | -2.60                 | 0.70               | 0.90                | 0.50                  | 23.06 | 9.70                  | 6.10               | 6.60                | 6.80                  |
| 20.09 | -0.30                 | 2.50               | 2.50                | 2.30                  | 23.09 | 6.00                  | 6.10               | 5.80                | 6.30                  |
| 20.12 | 1.70                  | 3.90               | 3.70                | 3.60                  | 23.12 | 5.00                  | 5.80               | 5.80                | 6.00                  |
| 21.03 | 17.60                 | 18.70              | 19.20               | 19.50                 | 24.03 | 5.00                  | 5.20               | 6.20                | 6.10                  |
| 21.06 | 12.70                 | 12.90              | 13.20               | 13.40                 | 24.06 | 4.80                  | 5.30               | 5.80                | 5.60                  |

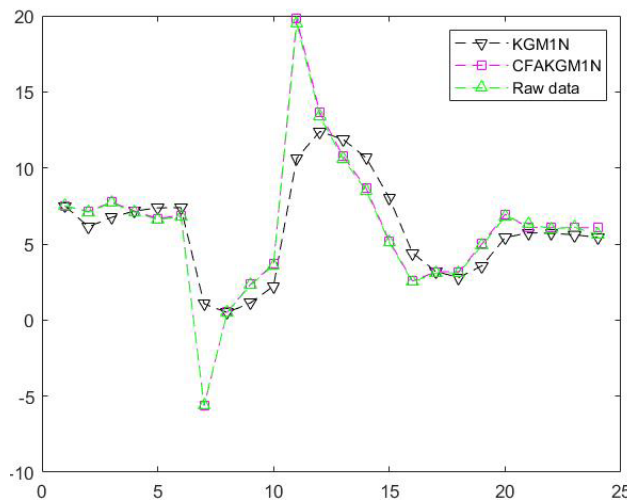


Figure 1: The scatter plots displaying the simulation and prediction outcomes of the two models.

As depicted in Figure 1, the fitting curve of KGM (1, N) roughly tracks the original data trend but shows slight inadequacy and bias when there are sharp changes in the data. In contrast, the fitting curve of CFAKGM (1, N) is smoother, particularly in areas with significant data fluctuations, demonstrating greater adaptability and overall better fitting effect.

In the realm of prediction, while the KGM (1, N) model can capture the fundamental trend of the data, it exhibits a substantial prediction error within regions of complex fluctuation. Conversely, the CFAKGM (1, N) model demonstrated enhanced stability, with a reduced error margin between the predicted and actual values, particularly in scenarios where the data experienced significant fluctuations, showcasing

an improved prediction performance.

Comparing the two graphs in Figure 2, the number of iterations of CFAKGM (1, N) model (left picture) tends to be stable after only 30 times, while that of KGM (1, N) (right picture) requires more times. It is not difficult to see that the former model has a better fitting effect.

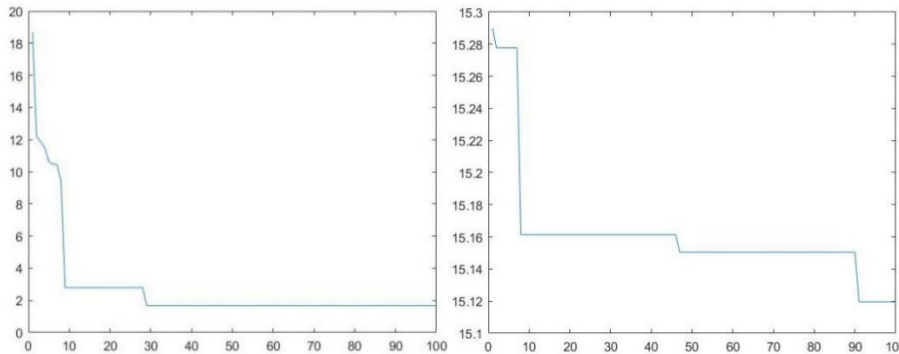


Figure 2: Convergence curve of the KGM model (Left picture) and CFAKGM model (Right picture).

Table 3: The simulation and prediction data of two models.

| Raw data                   | CFAKGM (1, N) | KGM (1, N) |
|----------------------------|---------------|------------|
| In-sample (simulation)     |               |            |
| 7.50                       | 7.50          | 7.50       |
| 7.10                       | 7.13          | 6.13       |
| 7.70                       | 7.76          | 6.75       |
| 7.10                       | 7.17          | 7.17       |
| 6.60                       | 6.68          | 7.37       |
| 6.80                       | 6.89          | 7.39       |
| -5.60                      | -5.65         | 1.06       |
| 0.50                       | 0.52          | 0.5        |
| 2.30                       | 2.35          | 1.13       |
| 3.60                       | 3.67          | 2.24       |
| 19.50                      | 19.81         | 10.63      |
| 13.40                      | 13.62         | 12.4       |
| 10.60                      | 10.79         | 11.87      |
| 8.50                       | 8.66          | 10.67      |
| 5.10                       | 5.20          | 8.02       |
| 2.50                       | 2.56          | 4.41       |
| 3.10                       | 3.17          | 3.19       |
| 3.10                       | 3.17          | 2.80       |
| 4.90                       | 5.01          | 3.56       |
| 6.80                       | 6.95          | 5.42       |
| Out-of-sample (prediction) |               |            |
| 6.30                       | 6.07          | 5.74       |
| 6.00                       | 6.07          | 5.70       |
| 6.10                       | 6.07          | 5.61       |
| 5.60                       | 6.07          | 5.43       |
| Mape                       |               |            |
| Sim-mape                   | 1.67          | 15.12      |
| Pre-mape                   | 3.24          | 6.25       |

As indicated by the simulation and predictive outcomes for the two models presented in Table 3, the CFAKGM (1, N) model exhibits significantly superior simulation and predictive accuracy compared to the KGM (1, N) model, with accuracy rates of 1.67% and 3.24%, respectively. This suggests that the CFAKGM (1, N) model is capable of precisely forecasting the cumulative GDP growth of Zhejiang Province.

## 6. Conclusion

Based on the chart data provided, this work deeply analyzes and compares the difference between KGM (1, N) and CFAKGM (1, N) models in the prediction performance. By objectively proving the consistency between the model predictions and the actual data, this work attempts to give a thorough and reliable basis for evaluating the performance of the two models. The chart data clearly show that CFAKGM (1, N) model has higher accuracy in prediction than KGM (1, N) model. The predicted lines are closer to the actual data, indicating that CFAKGM (1, N) has an advantage in capturing dynamic changes in data. The analysis based on the chart data shows that CFAKGM (1, N) model is dramatically better than KGM (1, N) model in forecasting performance. The discovery provides new solutions to prediction problems in complex systems and demonstrates the potential of the CFAKGM (1, N) model for practical applications. The analysis in this article is based on a specific data set, and the results may not apply to all types of data. In the future, it can be combined with other modeling techniques to test CFAKGM on different data types to further improve its performance.

## References

- [1] Zhang D, Luo D. *Research on the prediction model of agricultural drought hazard considering the time-delayed cumulative effect and system development characteristics [J]. Science of The Total Environment, 2023, 882: 163523.*
- [2] Sapnken F E, Ahmat K A, Boukar M, et al. *Forecasting petroleum products consumption in Cameroon's household sector using a sequential GMC (1, n) model optimized by genetic algorithms[J]. Heliyon, 2022, 8(12).*
- [3] Meng Z, Liu X, Yin K, et al. *Forecasting China's energy intensity by using an improved DVCGM (1, N) model considering the hysteresis effect[J]. Grey Systems: Theory and Application, 2021, 11(3): 372-393.*
- [4] Guo X, Wu L, Wang M. *Application of Grey Lotka-Volterra model in water-economy-industry-technology innovation system in Beijing-Tianjin-Hebei region[J]. International Journal of Environmental Research and Public Health, 2022, 19(15): 8969.*
- [5] Ma X, Liu Z. *The kernel-based nonlinear multivariate grey model[J]. Applied Mathematical Modelling, 2018, 56: 217-238.*
- [6] Khalil Roshdi, Al Horani M, Yousef Abdelrahman, Sababheh Mohammad. *A new definition of fractional derivative[J]. Comput Appl Math 2014; 264: 65–70.*
- [7] Xie M, Wu L, Li B, et al. *A novel hybrid multivariate nonlinear grey model for forecasting the traffic-related emissions[J]. Applied Mathematical Modelling, 2020, 77: 1242-1254.*
- [8] Hou H, Xu P, Zhou Z, et al. *Hardware error correction for MZI-based matrix computation[J]. Micromachines, 2023, 14(5): 955.*
- [9] Verma S, Boonsanong V, Hoang M, et al. *Counterfactual explanations and algorithmic recourses for machine learning: A review [J]. ACM Computing Surveys, 2020.*
- [10] Ma X, Wu W, Zeng B, et al. *The conformable fractional grey system model[J]. ISA transactions, 2020, 96: 255-271.*